Electrochimica Acta 268 (2018) 546–553

Contents lists available at ScienceDirect

Electrochimica Acta

journal homepage: www.elsevier.com/locate/electacta

Photoelectrochemical reactivity of well-defined mesoscale gold arrays on SiO_2/Si substrates in CO_2-saturated aqueous electrolyte

Simon Filser [a], Thomas L. Maier [a], Robin D. Nagel [b], Werner Schindler [a], Paolo Lugli [c], Markus Becherer [b], Katharina Krischer [a, *]

[a] Nonequilibrium Chemical Physics, Department of Physics, Technical University of Munich, James-Franck-Strasse 1, 85748 Garching, Germany
[b] Institute for Nanoelectronics, Department of Electrical and Computer Engineering, Technical University of Munich, Theresienstrasse 90, 80333 München, Germany
[c] Faculty of Science and Technology, Free University of Bolzano, piazza Universita, 5, Bolzano, Italy

ARTICLE INFO

Article history:
Received 17 October 2017
Received in revised form
29 January 2018
Accepted 3 February 2018

Keywords:
CO_2 reduction
Photoelectrochemistry
Metal-semiconductor interface

ABSTRACT

In this article we present a study on the influence of the size of mesoscopic gold nanostructures on silicon (Si) with well-defined geometry on their reactivity towards hydrogen evolution and carbon dioxide reduction. The onset potential for these two reactions decreases by 170 mV with structure size decreasing from 1400 nm to 75 nm, whereby hydrogen evolution is accelerated somewhat more than carbon dioxide reduction. This effect is independent of the doping type and level of the substrate, i.e. it occurred for moderately doped p-type Si (p-Si) under illumination, as well as on n-type (n-Si) and degenerately doped p-type Si (p^{++}-Si) in the dark. Therefore, the increase in reactivity is not influenced by the metal/semiconductor contact which changes from Schottky-type for p-Si to ohmic for p^{++}-Si. Due to the relatively large structure size, quantum confinement and a change in surface defect density do not play a role. We argue that the role of the metal structure edges, which increases with decreasing structure size, is decisive. At the edges, the electrostatic charge and potential distribution as well as the chemical environment are different compared to the conditions at the interior surface. At present it remains unclear whether the reactivity enhancement is predominantly due to an electrostatic effect or a chemical, bifunctional mechanism.

1. Introduction

Due to the need for regeneratively produced fuels and base chemicals, photoelectrochemical (PEC) water splitting [1–3] and carbon dioxide (CO_2) reduction [4–8] have drawn much attention in recent years. Yet, we are still far from an economically working fully integrated PEC device. The latter has to fulfill two base tasks: It has to provide a sufficiently high photovoltage to drive the electrochemical reaction and it has to allow for fast electron transfer at the electrode/electrolyte interface. Recent studies showed that silicon (Si) based multijunction cells can fulfill the requirements on the photovoltage, at least for water splitting [9–11]. Combining the high photoefficiency of such Si-based multijunction cells with high electrocatalytic activity towards water splitting or carbon dioxide (CO_2) reduction and improved stability with respect to electrocorrosion is therefore an attractive route towards a functional, integrated device.

One possible strategy is to decorate a stabilized Si surface with metal catalysts [4–6,12–16]. The stabilization can be achieved by covering the surface with a thin layer of silicon oxide or other passivating oxides, as e.g. $SrTiO_3$ [14]. In this way, metal/insulator/semiconductor (MIS) structures are formed. When illuminating a MIS photocathode, the light is absorbed in the semiconductor and photogenerated electrons tunnel through the insulating oxide layer to the electrocatalytically active metal structure, at which the electrochemical reaction takes place. Optimization of such a photoelectrode has again two aspects: optimizing the MIS contact and optimizing the electrochemical activity of the interface. This task is complicated by the fact that many properties of the interface affect both, the photovoltaic and the electrocatalytic performance. Metal/semiconductor contacts in the nm range are predicted to increase the photovoltage [12], but metal nanoparticles might also exhibit catalytic properties different from bulk substrates [17,18]. A way to

---

* Corresponding author.
E-mail address: krischer@tum.de (K. Krischer).

https://doi.org/10.1016/j.electacta.2018.02.018

disentangle the different contributions seems to be to carry out fundamental studies with well-defined structures with sizes well in the mesoscopic region, where the influence of size should be minimal. In the literature, arrays of regular metal structures are used [13–15], with a linear sizes ranging from 50 nm in Ref. [14] to a few hundred μm in Ref. [13]. The latter two publications observe an effect of increasing activity which is ascribed to an inversion channel for enhanced electron transport and to hydrogen spillover. Also nanoparticulate metal layers on Si with particle sizes ranging from a few hundred nm to a few ten nm were employed, the observed improved catalytic activity being ascribed to metal/semiconductor contact areas of just a few nm [12].

In this study, we investigate the activity of MIS photocathodes, with very regular metal arrays extending over macroscopic dimensions (several mm) and individual structure sizes between 1400 nm and 75 nm, aiming at making a contribution to the fundamental understanding of the influence of the metal structure size on the electrochemical reactivity of the photocathode. We thus did not put any effort in optimizing the electronic properties of the MIS structure, i.e. the photovoltage. The photocathodes are composed of Au/Ti/SiO_2/p-Si structures, and the electrolyte employed is a CO_2 saturated phosphate buffer, with water splitting and CO_2 reduction being competing reactions. In the following, we first describe the preparation of the photoelectrodes via lift-off nanoimprint lithography (LO-NIL) [19,20] and the details of the electrochemical measurements. In section 3, the photoelectrochemical measurements are presented and compared to n-Si and degenerately doped p-Si based MIS structures which exhibit electrochemical activity in the dark.

2. Experimental

2.1. Sample fabrication

The gold (Au) nanostructures are prepared on Si wafers with the following specifications:

n-type: CZ(100), $[P] = 1\cdot10^{15} - 5\cdot10^{15}$ cm^{-3}, $1 - 5$ Ωcm, double side polished, Microchemicals GmbH, Germany;

p-type: CZ(111), $[B] = 5\cdot10^{15} - 4\cdot10^{16}$ cm^{-3}, $5 - 25$ Ωcm, single side polished, Si-Mat, Germany;

degenerate p-type (p^{++}): CZ(111), $[B] > 1\cdot10^{19}$ cm^{-3}, < 0.01 Ωcm, single side polished, Si-Mat, Germany.

In the following, the different doping levels will be denoted as n-Si, p-Si and p^{++}-Si, respectively. The wafers were thermally oxidized for 8 min at 1000°C, resulting in a thermal oxide layer thickness of about 30 nm. To achieve an exact thickness of (15±1) nm the oxide was thinned down for 30–40 s in buffered oxide etch (BOE), a 98:2 mixture of 40% ammonium fluoride (NH_4F) and 50% hydrofluoric acid (HF) solution. This thermal oxide layer, which remained on the part of the surface not covered by Au nanostructures, proved to constitute a stable passivating layer preventing unwanted current flow over the SiO_2/Si interface over hours (see Fig. S2 in the SI).

The back side of the Si samples is prepared with an aluminum (Al) back contact, where first the oxide is removed by BOE with a mixing ratio of 6:1. Then, a 200 nm thick Al layer is deposited onto the etched surface via physical vapor deposition and subsequently annealed (n-Si: 250°C for 15 min, p-Si and p^{++}-Si: 400°C for 30 min) in vacuum.

The front side of the 11.5×11.5 mm^2 large samples is decorated with Au nanostructures on a square of 5×5 mm^2 using the LO-NIL fabrication method [19] which is summarized in the following: First a lift-off resist (LOR) (PMGI SF6, MicroChem Corp., USA) is spin-coated on the wafer and baked (3 min, 250 °C). Afterwards a thermal imprint polymer layer (MR-I8020R, micro resist technology GmbH, Germany) is directly spin-coated on top of the LOR and baked (1 min, 100 °C). The sample is now patterned in a thermal imprint process (3 min, 165 °C, 30 bar) using a nanopatterned stamp. Afterwards, an anisotropic reactive ion etching (RIE) step removes the thin imprint residual layer and a part of the LOR. In an isotropic wet-chemical developing step the imprint resist is underetched by using a 1:5 solution of AZ400K:DI water (Clariant GmbH, Germany). The partial removing of the LOR below the imprint resist results in an artificial undercut needed for the lift-off process. After underetching, a second anisotropic RIE step is applied to remove the thermal silicon oxide below the future Au nanostructures. This surface is again covered by plasma oxide with a thickness of (1.8 ± 0.2) nm in an additional plasma oxidation step.

The target metals (titanium (Ti) and Au) are deposited in a high vacuum physical vapor deposition system. First, a 3 nm thick Ti adhesion layer is evaporated under a pressure of $4\cdot10^{-8}$ mbar at a rate of 0.1 nm/s. Afterwards, a Au layer of (15±1) nm thickness is evaporated under a pressure of $8\cdot10^{-8}$ mbar with a rate of 0.3 nm/s.

The last step is the lift-off step which is done immersing the samples in 1-methyl-2-pyrrolidon (NMP) under ultrasonification until the sacrificial resist is completely removed and only the metal nanostructures remain on the substrate.

These nanostructured Au layers are complemented by continuous Au films on p-Si and n-Si which are evaporated in the way described above, but without imprint resist and thermal oxide, i.e. directly on a (1.8 ± 0.2) nm thick layer of plasma oxide. Also a 1 mm thick Au foil with a purity of 99.995% (Chempur Feinchemikalien und Forschungsbedarf GmbH, Germany) has been used as a bulk gold sample. A sketch of the sample design is given in Fig. 1, and scanning electron microscope (SEM) pictures of a fabricated nanostructure array and a single larger nanosquare are given in Fig. 2. Further SEM images of the other structure sizes can be found in the supplementary information (Fig. S1 in the SI). The important geometrical parameters of the nanosquares and nanodisks used are given in Table 1. Their structure size to pitch size ratio differs only slightly, and thus the percentage of the substrate surface area which is covered by metal. The deviations in the actual Au surface in contact with the electrolyte, which includes also the sides of the Au disks or Au squares, are somewhat larger, ranging between 22 and 28 %. One important geometrical parameter in which the sizes of the Au patches differ is the length of the circumference of the structure per unit area of Au, which is larger by a factor of about 24 for the smallest structure compared to the largest one.

2.2. Photoelectrochemical measurements

All electrochemical measurements shown here have been recorded using a three-compartment cell made of

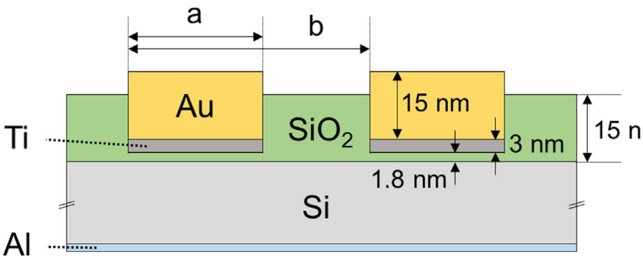

Fig. 1. Schematic sample design (not to scale). *a*: nanostructure diameter (between 1400 nm and 75 nm), *b*: pitch (*b*/*a* is between 2.0 and 2.15). Parameters which are numerically specified are constant for all samples.